European Polymer Journal 164 (2022) 110955

Contents lists available at ScienceDirect

European Polymer Journal

journal homepage: www.elsevier.com/locate/europolj

Wavelength-selective responsive hybrid structures utilizing shape memory poly(aryl ether ketone)

Shuai Yang [a], Yang He [a], Yanju Liu [b], Jinsong Leng [a,*]

[a] Center for Composites Materials and Structures, Harbin Institute of Technology, Harbin, PR China
[b] Department of Astronautic Science and Mechanics, Harbin Institute of Technology, Harbin, PR China

ARTICLE INFO

Keywords:
Wavelength-selective response
Shape memory poly(aryl ether ketone)
Deformable smart structures
Diverse programmable paths

ABSTRACT

Wavelength-selective responsive shape memory polymers (SMPs) are able to achieve significantly programmable deformations upon light irradiations with different wavelengths, which are expected to play the important roles in diverse smart devices. At present, the most of wavelength-selective responsive SMPs exhibit poor strength and thermo-stability, which restrict their utilizations in sensor and aerospace structures. Here, we constructed the light responsive poly(aryl ether ketone) (PAEK) hybrid structures with enhanced strength and wavelength-selective responses, which exhibited programmable multistage deformations under light irradiations of different wavelengths (365 nm and 254 nm). Besides, we designed "man" and "flower" smart structures with photo-responsive PAEK components to demonstrate wavelength-selective responsive motions. The smart "man" could spontaneously open his limbs and the "flower" could bloom via diverse programmable paths, which could be tuned by manipulating the arrangement of photosensitive components and light irradiation wavelengths. The wavelength-selective shape memory hybrid structures could be widely utilized in the fields of soft robots, smart actuators, and deformed devices.

1. Introduction

Shape memory polymers (SMPs), as smart materials, are able to retain the temporary shape and recover to the original shape upon external stimuli, such as heat, electricity, magnetic field, and light [1–4]. The active deformation ability imparts the plenty of applications, including aerospace manipulations, flexible electronics, soft robots, and smart actuators [5–10]. Conventional SMPs exhibit only one temporary shape in an independent shape memory cycle, named as dual shape memory effect, which significantly restricts their utilizations in complicated smart structures [11–13]. In addition, as the development of science and technology, selective responsive SMPs have attracted much attention, due to the unique regional selective shape memory behaviors [14,15]. These regional responsive SMPs could achieve diverse programmable shape recovery paths upon the sequenced external stimuli, which could achieve the programmability and selectivity [16,17].

The selective responsive SMPs could be constructed through integrating the different actuation modes, including heat, magnetic, electric and so on. [18–22]. Recently, photo-responsive SMPs have attracted great attention due to the environment adaptability, remote controlling, precise, and instantaneity [23–25]. At present, the two main mechanisms for photo-responsive SMPs are based on photo-thermal effect, and photosensitive reaction [26]. The former one includes the incorporation of photo-thermal fillers into heat-responsive SMPs, for instance of carbon materials (carbon black [27], carbon nanotubes [28], and graphene derivatives [29]), polydopamine [30], Au nanobars [31], and so on. These functional fillers which acting as photo-absorbers and heat sources are able to transform light energy into heat, and result in triggering the shape memory effect [32,33]. In this one, light is just the one kind of stimulus, and other responsive mechanisms have to be introduced into the SMPs that could achieve the target selective response. As for the latter, the photo-responsive shape memory effect originates from the reaction of photosensitive groups including azobenzene [34], coumarin [35], and cinnamic acid [36], into SMPs matrix. These groups are sensitive to photo irradiation of certain wavelength, and impart SMPs the photosensitivity. Upon the irradiation, the reaction among photosensitive groups occurs, and the internal stress stored before was released [37,38]. As a result, macroscopic shape recovery behaviors are triggered. It is noteworthy that photosensitive groups are response to the

Abbreviations: SMPs, Shape memory polymers; PAEK, poly(aryl ether ketone); ABZ, azobenzene; CA, cinnamic acid.

* Corresponding author.
E-mail address: lengjs@hit.edu.cn (J. Leng).

https://doi.org/10.1016/j.eurpolymj.2021.110955
Received 30 September 2021; Received in revised form 10 December 2021; Accepted 14 December 2021
Available online 18 December 2021
0014-3057/© 2021 Elsevier Ltd. All rights reserved.

irradiation of certain wavelength, nevertheless do not respond to other wavelength irradiation. Inspiringly, we could incorporate diverse groups that respond irradiation of different wavelength, to achieve target selective response. In this system, we utilize light as the only stimulus, except for different wavelength, which could be easily constructed and processed [39,40]. In addition, wavelength-selective responsive SMPs possess unique spatiality, wavelength discrimination and selectivity, and programming deformation and recovery, which have great utilization potential in field of accurate and complicated smart optical devices [41–45].

In this paper, we selected azobenzene groups as one of photosensitive groups which could occur the conformational transformation at λ of 365 nm and 520 nm, of cis- and *trans*-conformation. Carboxylation shape memory poly(aryl ether ketone) (PAEK-COOH) matrix was synthesized via a universal condensation polymerization, and azobenzene groups were grafted onto PAEK chains (PAEK-ABZ). The synthesized PAEK-ABZ exhibited the excellent photo-triggered shape memory effect upon the irradiation of λ of 365 nm. Besides, we employed cinnamic acid as the other photosensitive groups which could occur the cycloaddition at λ of 365 nm and ring-opening reaction at λ of 254 nm, and integrated it into shape memory PAEK matrix via a solution blending (PAEK/CA). Afterwards, we assembled PAEK-ABZ, PAEK, and PAEK/CA components into a whole construction, as depicted in Fig. 1. These composite structures exhibited excellent wavelength-selective shape memory effect, which could respond to the irradiation with λ of 365 and 254 nm, corresponding to PAEK-ABZ and PAEK/CA components.

2. Experimental

2.1. Materials

2,2-bis (3-amino-4-hydroxyphenyl) hexafluoropropane (BAHHF), 4,4′-(hexafluoroisopropylidene) diphenol (HFPD), 4,4′-difluorobenzophenone (DFBP), 4,4′-bis (4-hydroxyphenyl) valeric acid (BHVA), potassium carbonate (K_2CO_3), tetramethylene sulfone (TMSF), p-Aminoazobenzene (ABZ), dicyclohexylcarbodiimide (DCC), and cinnamic acid (CA) were purchased from Aladdin Industrial. Toluene and N-methyl kelopyrrolidide (NMP) were all bought from Tianjin Guangfu Chemical Reagent Factory.

2.2. Synthesis of PAEK-ABZ

We utilized a conventional condensation polymerization to synthesize PAEK-COOH, which was reported before [46]. Certain proportion of HFPD, DFBP, BHVA, and K_2CO_3 were added into TMSF/toluene mixed solvent, which was equipped with Dean-Stark trap and nitrogen atmosphere. The produced moisture was removed at 140 °C for 2 h, and the polymerization was carried out at 170 °C for 5 h. Afterwards, the viscous product was poured into isopropanol/distilled water mixture, and then the precipitate was rinsed for several times. The synthesized PAEK-COOH was dried in a vacuum oven at 80 °C for 24 h, and the reaction yield was 91%. It was noteworthy that the molar proportion of HFPD and BHVA was 9:1, and 7:3, corresponding to the PAEK-C1 and PAEK-C3, respectively.

The synthesized PAEK-COOH was added into NMP with vigorous stirring, and then certain amount of ABZ and DCC were added into solution. The reaction was carried out at 40 °C for 15 h. The synthesized PAEK-ABZ solution was poured into propanol/distilled water mixture, rinsed for several times, and dried for 24 h. The proportion of carboxyl groups and ABZ was 1:1, 1:0.5, and 1:0.25, calling as PAEK-ABZ1, PEAK-ABZ0.5, and PAEK-ABZ0.25, respectively. The fabrication strategy and synthesis pathway of PAEK-ABZ are showed in Fig. 2. Shape memory PAEK-COOH was synthesized via a universal condensation polymerization. The benzene groups in main chains, crystalline phase, and chains entanglement acted as stationary phase, and the flexible segments including carbon bonds, ether and ketone groups acted as reversible phase. These combination of stationary and reversible phases imparted the excellent shape memory effect. After the grafting of ABZ groups onto molecular chains, the photo-responsive shape memory effect could be achieved via the photo-isomerization of ABZ groups, which transformed from *trans*-conformation into *cis*-conformation while irradiating at λ of 365 nm.

2.3. Preparation of PAEK-ABZ, PAEK, and PAEK/CA composite films

The synthetic pathway of PAEK were introduced in Supplement

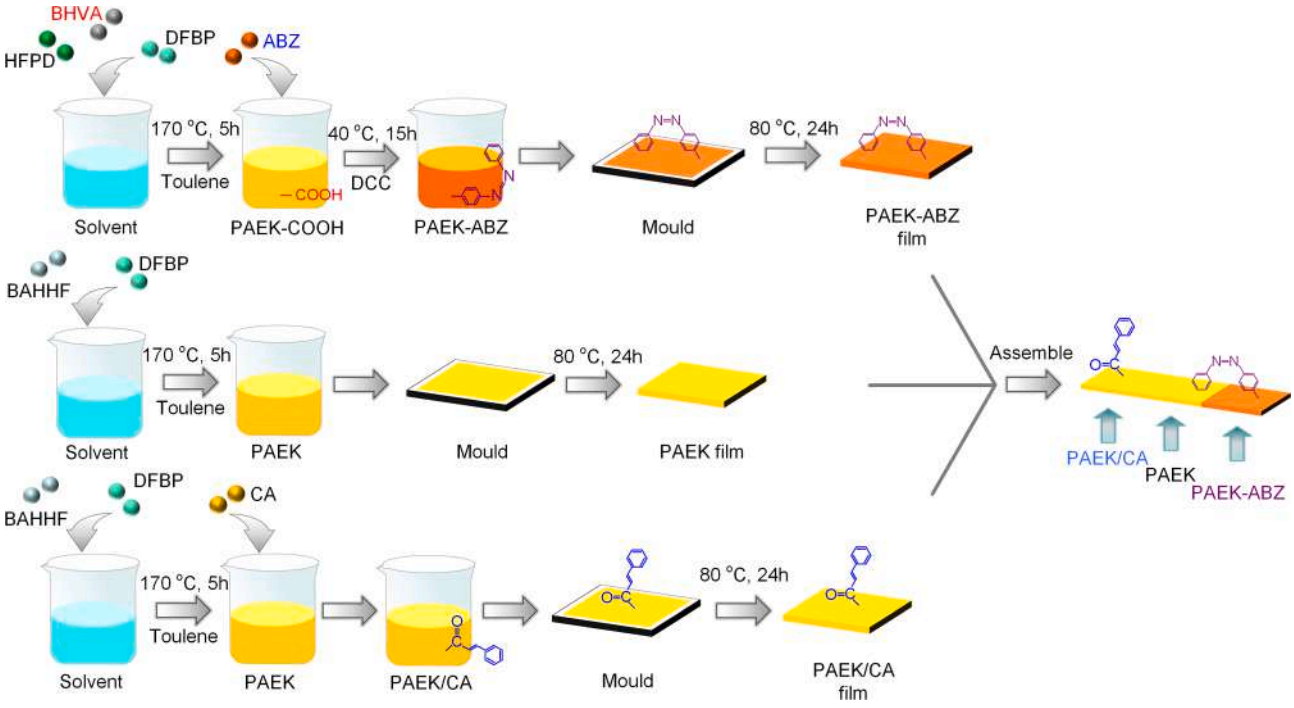

Fig. 1. Fabrication route of wavelength-selective responsive shape memory PAEK films.

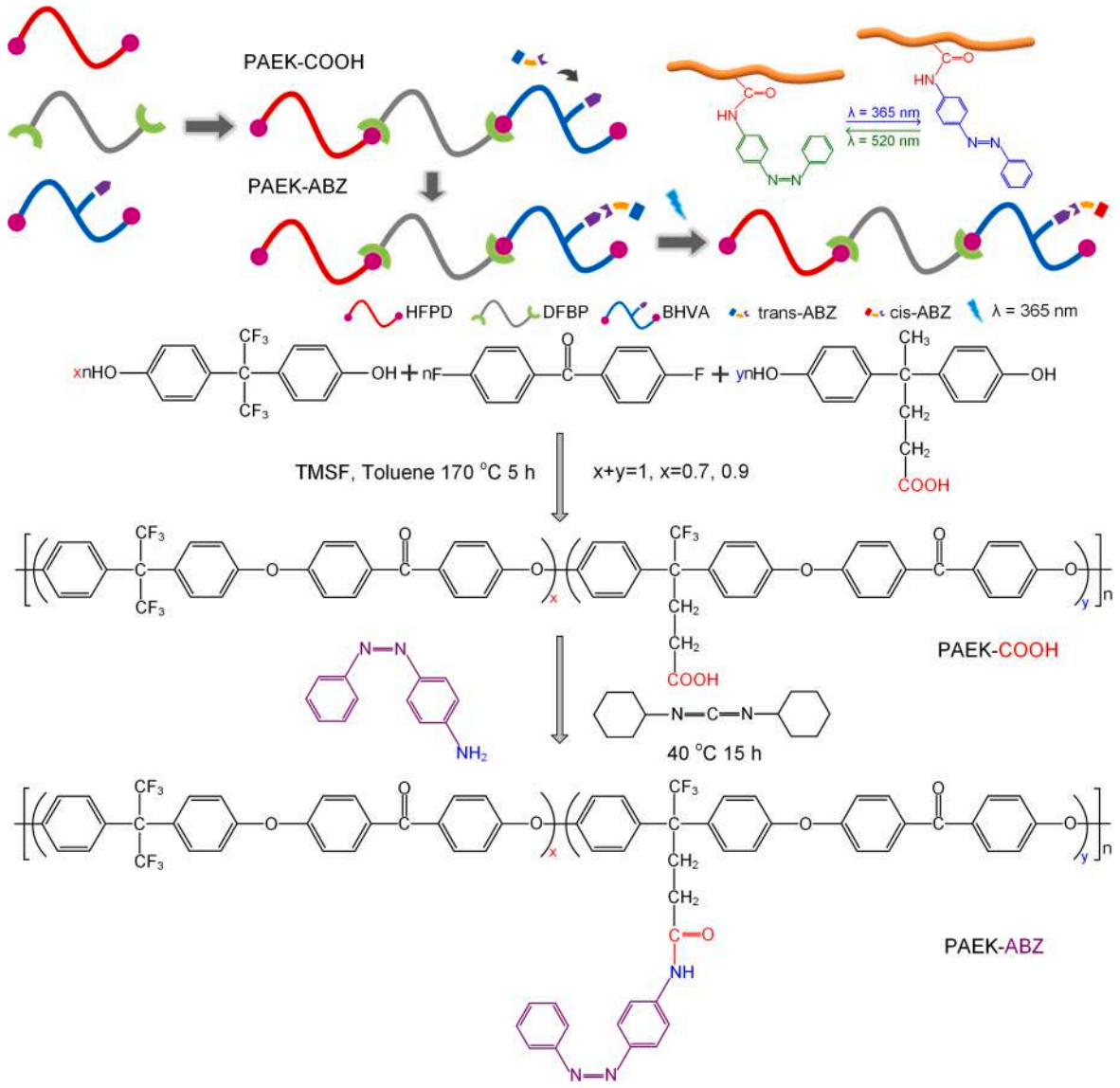

Fig. 2. Fabrication strategy and synthesis pathway of PAEK-ABZ.

Information. PAEK-ABZ and PAEK were independently dissolved into NMP with vigorous stirring. Then, certain amount of CA was added into PAEK solution under stirring. Afterwards, the prepared solutions were cast into homemade moulds and dried at 80 °C for 48 h. The prepared films were peeled off from moulds, and the molar proportion of PAEK and CA was 1:1.

2.4. Characterization

We utilized ^{1}H-nuclear magnetic resonance (^{1}H NMR) spectra (ADVANCE III 400 MHZ 010,601 spectrometer (Bruker)) to characterize the chemical structures of PAEK-COOH and PAEK-ABZ. $CDCl_3$ was used as the solvent and tetramethylsilane (TMS) was used as the internal reference. Fourier transform infrared (FTIR) spectroscopy was recorded by a Spectrum Two (PerkinElmer). Wide-angle (WAXD) patterns were recoreded on a X'pert XRD analyzer (Panalytical B.V.). The 2θ range was 5°-55°, and a step size was 10°/min. UV–vis absorption spectra was performed on a Mettler Toledo UV7 spectrophotometer.

2.5. Photo-triggered shape memory test

PAEK-ABZ film was deformed into a temporary shape by external force after heating, and then treated with UV irradiation with λ of 365 nm for the actuation of shape recovery. PAEK/CA film was deformed into a temporary shape by external force upon the irradiation with λ of 365 nm, and then treated with UV irradiation with λ of 254 nm, triggering to the shape recovery. The whole shape recovery processes were recorded by a digital camera.

3. 3. Results and discussion

3.1. Structures and mechanical performances

^{1}H NMR spectra of synthesized PAEK-COOH and PAEK-ABZ is showed in Fig. 3a. The chemical shifts at 7.84 ppm, 7.43 ppm, and 7.09 ppm were corresponding to the protons of 3, 2, and 1, respectively. The chemical shifts of the protons on BHVA were at 1.62 ppm, 2.24 ppm, and 3.05 ppm, corresponding to the protons of 4, 5, and 6. Nevertheless, the chemical shift of proton signal for the carboxylic groups was not occurred, which was concerned with the reaction between active hydrogen protons and $CDCl_3$ solvent. We utilized *d*imethylsulfoxide-d_6 (DMSO-d_6) as solvent to characterize PAEK-C1, which exhibited the chemical shift of proton of carboxylic groups, shown in Fig. S1. After the grafting of ABZ, the chemical shifts of protons in ABZ groups ranged

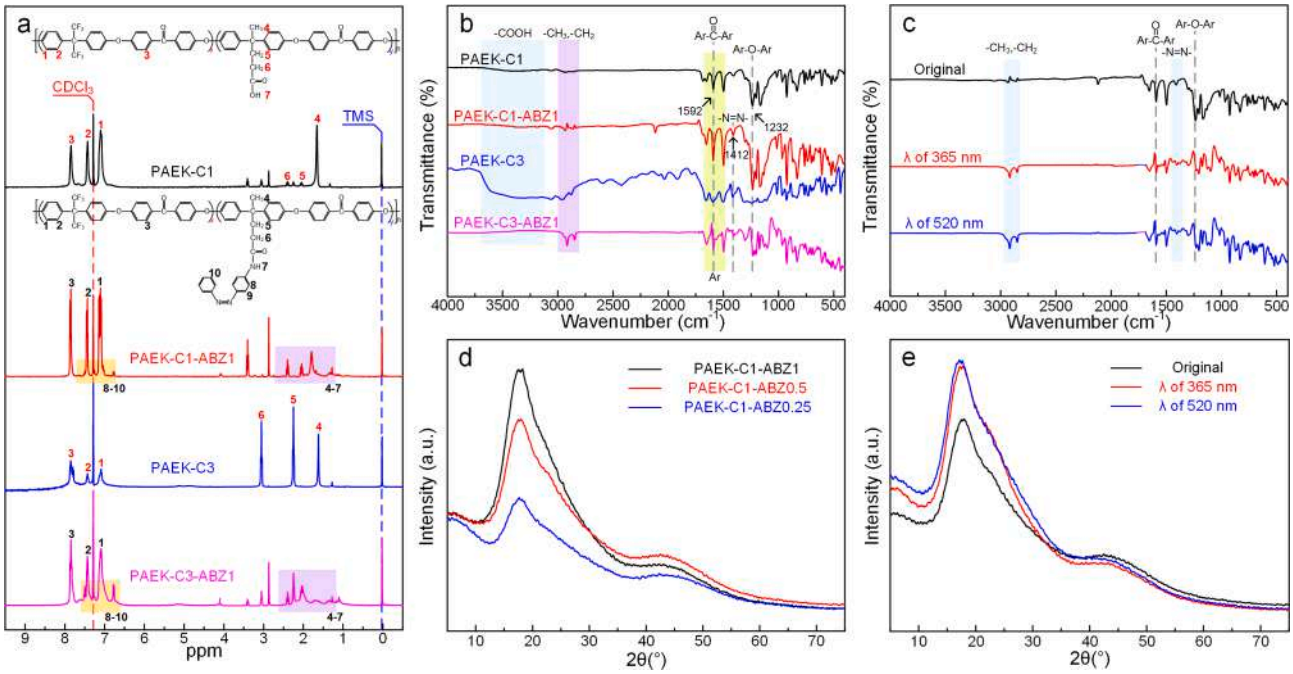

Fig. 3. (a) ^{1}H NMR spectra of PAEK-COOH and PAEK-ABZ; FTIR spectra of (b) PAEK-COOH and PAEK-ABZ, and (c) PAEK-C1-ABZ1 with UV irradiation; XRD curves of (d) PAEK-ABZ, and (e) PAEK-C1-ABZ1 with UV irradiation.

from 1.22 ppm to 2.71 ppm, corresponding to the protons of 4, 5, 6, and 7. Besides, from 6.69 ppm to 7.61 ppm, the chemical shifts occurred, concerning with the protons of 8, 9, and 10. FTIR spectra is showed in Fig. 3b. The peaks at the range from 3231 cm^{-1} to 3610 cm^{-1} were corresponding to the characteristic peak of carboxylic groups. The PAEKs at 1592 cm^{-1} and 1232 cm^{-1} were concerned with aryl ether and carbonyl groups, respectively. After the incorporation of ABZ, the peaks at 1412 cm^{-1} occurred, which was attributed to the N = N bonds. FTIR spectra of PAEK-C1-ABZ1 treated with irradiation of diverse wavelength is depicted in Fig. 3c. It could be observed that while treated with the irradiation of λ of 365 nm and 520 nm, the peak position did not change, indicating that the photosensitive reaction of ABZ was just conformational transformation, rather than chemical reaction. WAXD curves of PAEK-ABZ are performed in Fig. 3d, which indicating to the semi-crystalline structures. As the deceasing of ABZ proportion, the characteristic peak became wider and smoother, indicating the decreasing crystalline. Fig. 3e performs the XRD curves of PAEK-C1-ABZ1 treated with irradiation of diverse wavelength. After the irradiation, the characteristic peak became narrower and sharper, indicating the increasing crystalline.

UV–vis spectra of PAEK-ABZ is showed in Fig. 4a. We could observe that the absorption peak of 306 nm for the *trans*-azobenzene chromophore are found in all three types of PAEK-ABZ. In Fig. 4b, after irradiating at λ of 365 nm for 20 min, the peak at 306 nm became lower, indicating the transition from *trans*-azobenzene to *cis*-azobenzene. When irradiated at λ of 520 nm, the peak became sharper again, concerning with the cis–trans azobenzene transition. Fig. 4c shows different treated time on PAEK-ABZ0.5 at λ of 365 nm. Increasing the treated time, the peak at 306 nm became lower. In addition, samples those treated at λ of 365 nm were irradiated at λ of 520 nm for different time, depicted in

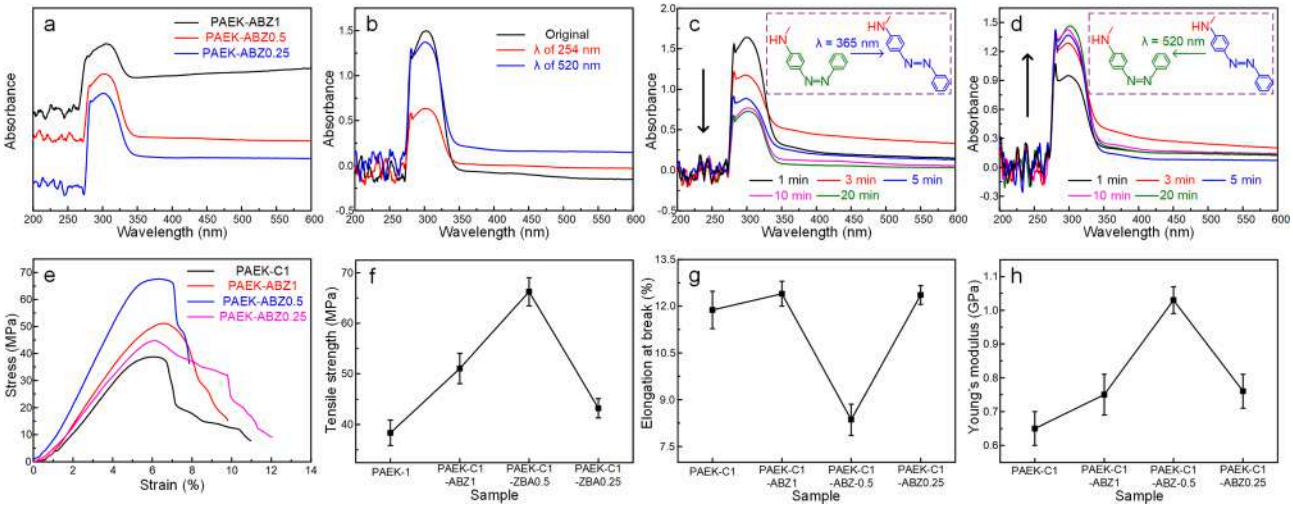

Fig. 4. UV–vis spectra of (a) PAEK-ABZ; (b) PAEK-ABZ0.5 treated with the irradiation with λ of 365 nm and 520 nm for 20 min; (c) Different treatment time on PAEK-ABZ0.5 at λ of 365 nm; (d) Different treatment time on PAEK-ABZ0.5 at λ of 365 nm and 520 nm; Mechanical performances of PAEK-C1 and PAEK-C1-ABZ (e) Stress–strain curves; (f) Tensile strength; (g) Elongation at break; (h) Young's modulus.

Fig. 4d. We could observe that as the increasing of treated time, the peak at 306 nm became sharper, indicating the transition from *cis*-azobenzene to *trans*-azobenzene. The mechanical performances of PAEK-C1 and PAEK-ABZ are depicted in Fig. 4e-h. In Fig. 4e, we could observe that the all the samples exhibited ductile fracture. In Fig. 4f, the tensile strength of PAEK-C1 was 38.4 MPa, which increased after the grafting of ABZ. The tensile strength of was 51.1 MPa when the molar proportion of PAEK and ABZ was 1:1. Then, when the proportion was 1:0.5, the tensile strength significantly increased, of 66.2 MPa, which might be concerned with the plasticization of excess unreacted ABZ monomers. Nevertheless, the tensile strength of PAEK-C1-ABZ0.25 was 43.2 MPa, just a bit higher than PAEK-C1. It was due to that the enhancement of the fewer ABZ rigid monomers on PAEK-C1 was not so significant. In Fig. 4g, the elongation at break of PAEK-C1, PAEK-C1-ABZ1, PAEK-C1-ABZ0.5, and PAEK-C1-ABZ10.25 was 11.9%, 12.4%, 8.36%, and 12.4%, respectively. Meanwhile, the Young's modulus of PAEK-C1, PAEK-C1-ABZ1, PAEK-C1-ABZ0.5, and PAEK-C1-ABZ10.25 was 0.65 GPa, 0.75 GPa, 1.03 GPa and 0.76 GPa, respectively, shown in Fig. 4h.

3.2. Photo-responsive shape memory behaviors

The photo-responsive shape memory effect of PAEK-ABZ film is depicted and demonstrated in Fig. 5. Fig. 5a shows the photo-responsive shape memory behaviors of PAEK-C1-ABZ0.5 film. Firstly, the sample with original "—" shape was heated and deformed to "N" shape, then the temporary shape was fixed under cooling. Afterwards, the sample with temporary "N" shape was irradiated at λ of 365 nm. After twenty minutes, the right part recovered to the original "—" shape, but the left one did not, which might be attributed to that vertical UV irradiation could not fully treat the left part. In Fig. 5b, as the decreasing of ABZ proportion, the shape recovery ratio of PAEK-ABZ film gradually decreased, from 85.2% to 81.6% and 76.3%, corresponding to the proportion of PAEK and ABZ of 1:1, 1:0.5, and 1:0.25, respectively. The photosensitive ABZ groups was triggered upon the irradiation to result in the macroscopic shape recovery. Of course, the increasing of proportion of ABZ would improve the shape recovery ability of sample. In Fig. 5c, as the decreasing of ABZ proportion, the fixity ratio decreased gradually decreased, from 98.3% to 97.5% and 95.5%, corresponding to PAEK-C1-ABZ1, PAEK-C1-PAEK0.5, and PAEK-C1-ABZ0.25, respectively. The fixity ratio of all the samples were over 95%, which was attributed to that the incorporation of rigid ABZ monomers improved the shape fixity ability. The mechanism of photo-responsive shape memory effect is showed in Fig. 5d. Usually, ABZ groups was in *trans*-conformation due to the better stability compared to *cis*-conformation. While the sample was heated and deformed by external force, the temporary shape could be obtained, but the *trans*-conformation was not changed. When the sample was irradiated at λ of 365 nm, the *trans*-conformation of ABZ would transform to *cis*-conformation. In this process of conformational transformation, the internal stress stored in deformation before was released, and then, shape recovery behaviors were triggered. In addition, we incorporated origami technique, as a kind of traditional culture, into shape memory PAEK-ABZ, and fabricated reversible fence and Pyramid origami structures, as depicted in Fig. 5e. Initially, we fabricated desired through-line patterns onto PAEK-ABZ square film, which was as the original shape. Subsequently, the film sample was heated and deformed into pre-designed fence and Pyramid structures by the external force. Afterwards, we utilized the irradiation with λ of 365 nm to treat with the film shape, and then, we observed the occurrence of shape recovery.

3.3. Wavelength-selective actuation of shape memory structures

Based on the investigation on PAEK-ABZ mentioned before, we employed PAEK-C1-ABZ1 as one of photosensitive components for the subsequent investigation which could be triggered by the irradiation with λ of 365 nm. Besides, we utilized PAEK/CA as the other photosensitive components which was responsive to the irradiation with λ of 365 nm and 254 nm, responding for shape fixity and recovery, respectively. Finally, we used PAEK to bridge two components, and then constructed wavelength-selective shape memory structures, depicted in Fig. 6a. Heating the right PAEK-ABZ component, and it was deformed into temporary shape by external force. Cooling the temperature and the temporary shape was fixed. Subsequently, we utilized irradiation with λ of 365 nm to treat the sample. In this process, we deformed the left PAEK/CA component by external force, and meanwhile, we observed the right PAEK-ABZ component spontaneously recovered to the original shape. Finally, the irradiation of the sample with λ of 254 nm resulted in the shape recovery of the left PAEK/CA component to the original shape. Besides, programmable diverse deformations could be achieved via the corresponding patterned manipulations, depicted in Fig. S2a,b. Fabricated wavelength selective responsive shape memory structures possessed great utilization potential, and we fabricated wavelength selective responsive "man" and "flower" which could act as controlling by irradiation, as depicted in Fig. 6b,c. In Fig. 6b, a smart "man" bended his arms and legs by external force after heating to arms and irradiating at λ of 365 nm to legs. Subsequently, he automatically opened his arms while irradiated at λ of 365 nm. Finally, he straightened his legs while irradiated at λ of 254 nm. The "man" opened his limbs in order of "arms to legs" while irradiated at λ of 365 nm and 254 nm. Besides, we transformed the action order of "man", from "arms to legs" to "legs to arms", depicted in Fig. S2c. He straightened his legs firstly while irradiated at λ of 365 nm, and then opened his arms while irradiated at λ of 254 nm. In Fig. 6c, a smart "flower" closed its petals by external force upon the corresponding heating and irradiation at λ of 365 nm. Then, it bloomed orderly its petals while irradiated at λ of 365 nm and 254 nm. Besides, we could change the blooming order of the petals by tuning the arrangement of petals, shown in Fig. S2d. Furthermore, we utilized homemade PAEK film as a substrate, and then integrated PAEK-ABZ and PAEK/CA components onto the substrate recording to the programming arrangement. The spontaneous shape recovery behaviors could deliver purposeful signals which could be determined by external irradiation and arrangement of photo-responsive components, shown in Fig S3. Fig. S4 shows several types of customized signal indicators which could deliver signals upon the external irradiation. The diverse customized actions of the "man", "flower" and "signal indicators" implied the great utilization value of these wavelength selective responsive shape memory structures in field of complicated smart devices, for instance of deformable bridge (Fig. S5).

3.4. Mechanism

The working mechanism of wavelength-selective shape memory structures is depicted in Fig. 7. Initially, the sample was of original shape, and then, the right PAEK-ABZ component was deformed into temporary shape by external force while heating. In this procedure, ABZ groups maintained the stable *trans*-conformation. Subsequently, the sample was irradiated at λ of 365 nm, where the conformational transformation occurred at ABZ groups, from *trans*-conformation to *cis*-conformation. In this process, the internal stress stored before was released, and shape recovery occurred. Meanwhile, the left PAEK/CA was deformed into temporary shape by external force, where cycloaddition occurred between the adjacent CA groups. Afterwards, we utilized irradiation with λ of 254 nm treated the sample, and the de-crosslinking reaction occurred at CA groups. As a result, the internal stress was released and shape recovery occurred.

4. Conclusions

In summary, we have developed wavelength-selective shape memory PAEK hybrid structures, and utilized them to construct diverse smart devices. ABZ groups were firstly grafted onto the molecular chains before the synthesis of shape memory PAEK-COOH via a conventional condensation polymerization. The photo-responsive shape memory

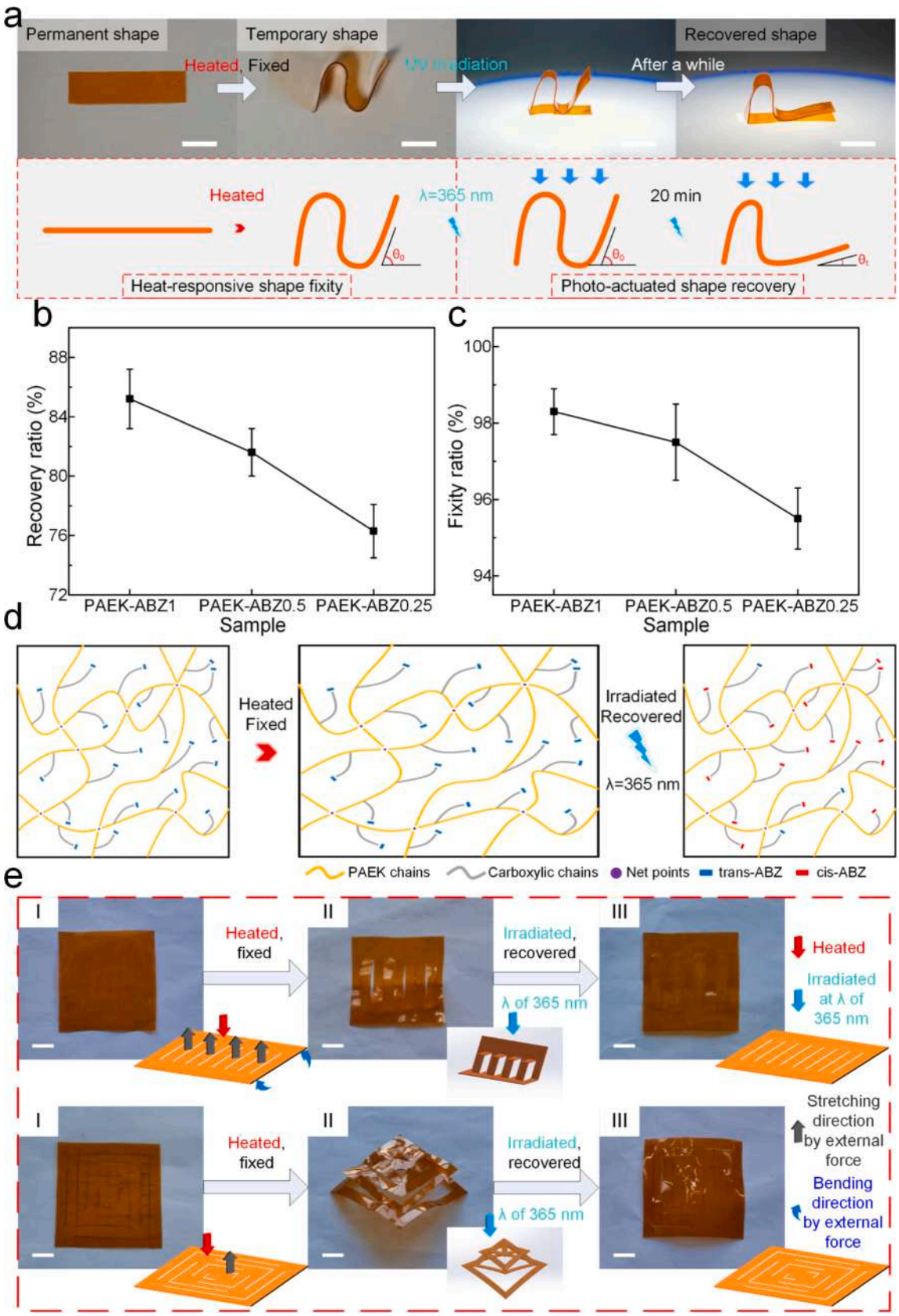

Fig. 5. (a) Photo-responsive shape memory behaviors of PAEK-C1-ABZ0.5; (b) Shape recovery ratio; (c) Fixity ratio; (d) Mechanism of photo-responsive shape memory effect; (e) Reversible fence and Pyramid origami patterns (scale bars of 1 cm).

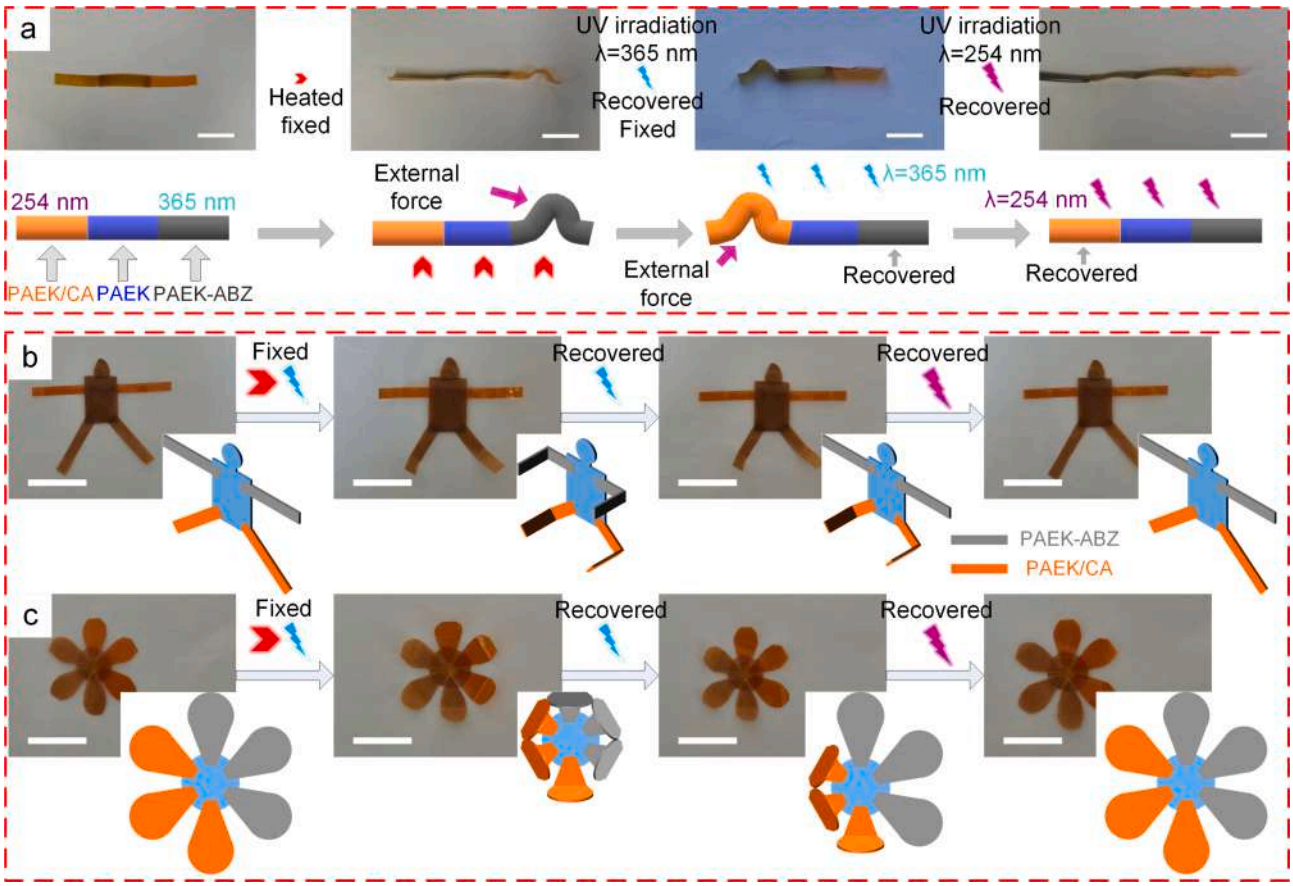

Fig. 6. (a) Wavelength-selective shape memory structures based on PAEK/CA, PAEK, and PAEK-ABZ components; (b) Smart "man" and (c) "flower" with their diverse customized actions (scale bars of 3 cm).

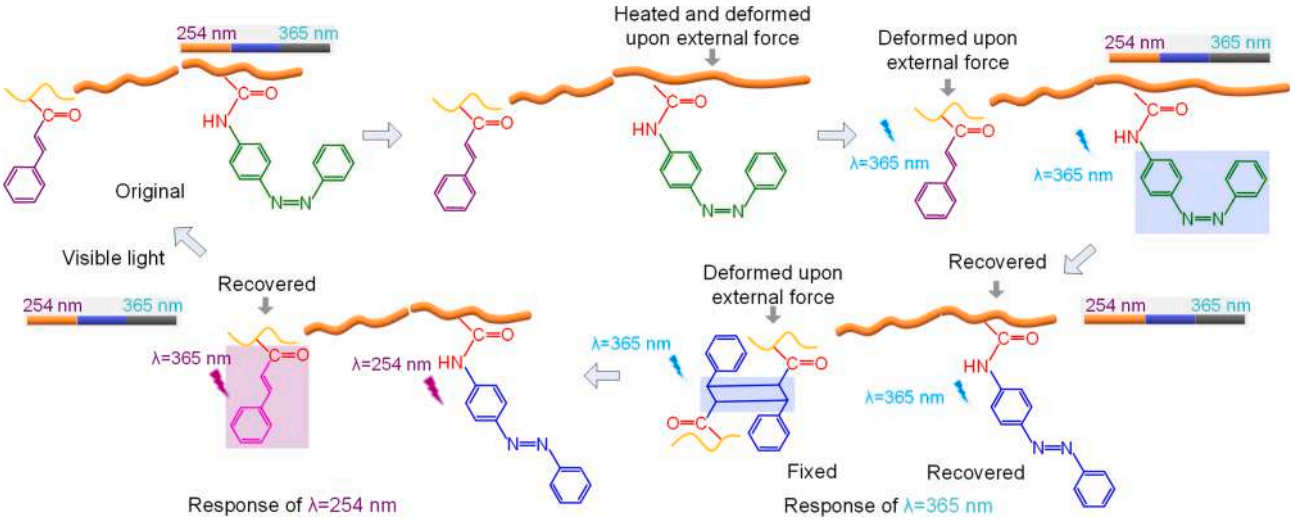

Fig. 7. Recovery mechanism of wavelength-selective responsive shape memory structures.

effect of PAEK-ABZ was investigated, and the results indicated that with the increasing of proportion of ABZ, both recovery ratio and fixity ratio gradually increased. Due to the advantage of easy-processing, we utilized PAEK-C1-ABZ1 as PAEK-ABZ component, for the subsequent investigation. Besides, we selected CA groups as the other photosensitive component, and prepared PAEK/CA composites which responded to the irradiation with λ of 365 nm and 254 nm. Afterwards, we assembled PAEK/ABZ, PAEK, and PAEK/CA components and constructed wavelength-selective shape memory hybrid structures. While irradiated at different wavelength (365 nm and 254 nm), the corresponding region could respond and spontaneously recover to the original shape. The hybrid structures achieved wavelength selective regional shape memory behaviors. In addition, we fabricated a smart "man" and "flower" based on these hybrid structures. Through the shape fixity and programming irradiation procedures, it was in diverse orders that the "man" opened his limbs and the "flower" bloomed. We could

tune the deformation actions via regulating the arrangement of components and manipulating the irradiation with different wavelength. Besides, we constructed wavelength-selective responsive signal indicators, which could deliver different information upon the irradiation with different wavelength. The setting and arrangement of individual signal indicators could be customized and pre-designed to achieve diverse signal delivering. We faithfully believed these wavelength selective responsive hybrid structures possessed great utilization potential in fields of soft robots, smart actuators, sensors, and devices.

Declaration of Competing Interest

The authors declare that they have no known competing financial interests or personal relationships that could have appeared to influence the work reported in this paper.

Acknowledgement

This work is supported by the National Natural Science Foundation of China (Grant No. 11632005).

Appendix A. Supplementary data

Supplementary data to this article can be found online at https://doi.org/10.1016/j.eurpolymj.2021.110955.

References

[1] J.M. Korde, B. Kandasubramanian, Naturally biomimicked smart shape memory hydrogels for biomedical functions, Chem. Eng. J. 379 (2020) 122430, https://doi.org/10.1016/j.cej.2019.122430.
[2] J. Xue, T. Wu, Y. Dai, Y. Xia, Electrospinning and Electrospun Nanofibers: Methods, Materials, and Applications, Chem. Rev. 119 (8) (2019) 5298–5415.
[3] P. Chakma, D. Konkolewicz, Dynamic Covalent Bonds in Polymeric Materials, Angew. Chem. Int. Edit. 58 (29) (2019) 9682–9695.
[4] Y.F. Zhang, N. Zhang, H. Hingorani, N. Ding, D. Wang, C. Yuan, B. Zhang, G. Gu, Q. i. Ge, Fast-Response, Stiffness-Tunable Soft Actuator by Hybrid Multimaterial 3D Printing, Adv. Funct. Mater. 29 (15) (2019) 1806698, https://doi.org/10.1002/adfm.v29.1510.1002/adfm.201806698.
[5] A. Lendlein, O.E.C. Gould, Reprogrammable recovery and actuation behaviour of shape-memory polymers, Nat. Rev. Mater. 4 (2) (2019) 116–133.
[6] X. Kuang, D.J. Roach, J. Wu, C.M. Hamel, Z. Ding, T. Wang, M.L. Dunn, H.J. Qi, Advances in 4D Printing: Materials and Applications, Adv. Funct. Mater. 29 (2) (2019) 1805290, https://doi.org/10.1002/adfm.v29.210.1002/adfm.201805290.
[7] X. Wang, X. Guo, J. Ye, N. Zheng, P. Kohli, D. Choi, Y.i. Zhang, Z. Xie, Q. Zhang, H. Luan, K. Nan, B.H. Kim, Y. Xu, X. Shan, W. Bai, R. Sun, Z. Wang, H. Jang, F. Zhang, Y. Ma, Z. Xu, X. Feng, T. Xie, Y. Huang, Y. Zhang, J.A. Rogers, Freestanding 3D Mesostructures, Functional Devices, and Shape-Programmable Systems Based on Mechanically Induced Assembly with Shape Memory Polymers, Adv. Mater. 31 (2) (2019) 1805615, https://doi.org/10.1002/adma.v31.210.1002/adma.201805615.
[8] J. Shintake, V. Cacucciolo, D. Floreano, H. Shea, Soft Robotic Grippers, Adv. Mater. 30 (29) (2018) 1707035, https://doi.org/10.1002/adma.v30.2910.1002/adma.201707035.
[9] X. Zhao, B.L. Guo, H. Wu, Y.P. Liang, P.X. Ma, Injectable antibacterial conductive nanocomposite cryogels with rapid shape recovery for noncompressible hemorrhage and wound healing, Nat. Commun. 9 (2018) 2784.
[10] T. Chen, O.R. Bilal, K. Shea, C. Daraio, Harnessing bistability for directional propulsion of soft, untethered robots, P. Natl. Acad. Sci. USA 115 (22) (2018) 5698–5702.
[11] Z. Deng, Y.i. Guo, X. Zhao, P.X. Ma, B. Guo, Multifunctional Stimuli-Responsive Hydrogels with Self-Healing, High Conductivity, and Rapid Recovery through Host-Guest Interactions, Chem. Mater. 30 (5) (2018) 1729–1742.
[12] R. Liu, X. Kuang, J. Deng, Y.C. Wang, A.C. Wang, W. Ding, Y.C. Lai, J. Chen, P. Wang, Z. Lin, H.J. Qi, B. Sun, Z.L. Wang, Shape Memory Polymers for Body Motion Energy Harvesting and Self-Powered Mechanosensing, Adv. Mater. 30 (8) (2018) 1705195, https://doi.org/10.1002/adma.v30.810.1002/adma.201705195.
[13] B. Jin, H. Song, R. Jiang, J. Song, Q. Zhao, T. Xie, Programming a crystalline shape memory polymer network with thermo- and photo-reversible bonds toward a single-component soft robot, Sci. Adv. 4 (1) (2018), https://doi.org/10.1126/sciadv.aao3865.
[14] Y.Z. Li, M. Goswami, Y.H. Zhang, T. Liu, J.W. Zhang, M.R. Kessler, L.W. Wang, O. Rios, Combined light- and heat-induced shape memory behavior of anthracene-based epoxy elastomers, Sci. Rep. 10 (2020) 20214.
[15] P.J. Feng, C.Q. Zhang, H.Y. Liang, D.S. Liang, Z.R. Lin, Q. Chen, Q.W. Wang, Renewable Castor Oil based Waterborne Polyurethane Networks: Simultaneously Showing High Strength, Self-healing, Processability and Tunable Multi-shape Memory, Angew. Chem. Int. Edit. 132 (2020) 2–13.
[16] W.S. Miao, W.K. Zou, B.J. Jin, C.J. Ni, N. Zheng, Q. Zhao, T. Xie, On demand shape memory polymer via light regulated topological defects in a dynamic covalent network, Nat. Commun. 11 (2020) 4257.
[17] Q. Zhou, X. Dong, Y. Xiong, B. Zhang, S. Lu, Q. Wang, Y. Liao, Y. Yang, H. Wang, Multi-Responsive Lanthanide-Based Hydrogel with Encryption, Naked Eye Sensing, Shape Memory, Self-Healing, and Antibacterial Activity, ACS Appl. Mater. Inter. 12 (25) (2020) 28539–28549.
[18] K.R. Ryan, M.P. Down, C.E. Banks, Future of additive manufacturing: Overview of 4D and 3D printed smart and advanced materials and their applications, Chem. Eng. J. 403 (2021) 126162, https://doi.org/10.1016/j.cej.2020.126162.
[19] Z. Shen, F. Chen, X. Zhu, K.-T. Yong, G. Gu, Stimuli-responsive functional materials for soft robotics, J. Mater. Chem. B 8 (39) (2020) 8972–8991.
[20] F. Zhang, Y. Xia, Y. Liu, J. Leng, Nano/microstructures of shape memory polymers: from materials to applications, Nanoscale Horiz. 5 (8) (2020) 1155–1173.
[21] C. Ma, S. Wu, Q. Ze, X. Kuang, R. Zhang, H.J. Qi, R. Zhao, Magnetic Multimaterial Printing for Multimodal Shape Transformation with Tunable Properties and Shiftable Mechanical Behaviors, ACS Appl. Mater. Interfaces 13 (11) (2021) 12639–12648.
[22] S. Pringpromsuk, H. Xia, Q.-Q. Ni, Multifunctional stimuli-responsive shape memory polyurethane gels for soft actuators, Sensor. Actuat. A-Phys. 313 (2020) 112207, https://doi.org/10.1016/j.sna.2020.112207.
[23] H.e. Xiao, W. Lu, X. Le, C. Ma, Z. Li, J. Zheng, J. Zhang, Y. Huang, T. Chen, A multi-responsive hydrogel with a triple shape memory effect based on reversible switches, Chem. Commun. 52 (90) (2016) 13292–13295.
[24] H.-Z. Wang, H.-F. Chow, A photo-responsive poly(amide-triazole) physical organogel bearing azobenzene residues in the main chain, Chem. Commun. 54 (60) (2018) 8391–8394.
[25] J.A. Lv, W. Wang, W. Wu, Y. Yu, A reactive azobenzene liquid-crystalline block copolymer as a promising material for practical application of light-driven soft actuators, J. Mater. Chem. C. 3 (26) (2015) 6621–6626.
[26] Y. Yang, Y. Yang, S.M. Chen, Q.C. Lu, L. Song, Y. Wei, X. Wang, Atomic-level molybdenum oxide nanorings with full-spectrum absorption and photoresponsive properties, Nat. Commun. 8 (2017) 1559.
[27] H. Yang, W.R. Leow, T. Wang, J. Wang, J. Yu, K.e. He, D. Qi, C. Wan, X. Chen, 3D Printed Photoresponsive Devices Based on Shape Memory Composites, Adv. Mater. 29 (33) (2017) 1701627, https://doi.org/10.1002/adma.v29.3310.1002/adma.201701627.
[28] X.D. Qi, Y.-W. Shao, H.Y. Wu, J.H. Yang, Y. Wang, Flexible phase change composite materials with simultaneous light energy storage and light-actuated shape memory capability, Compos. Sci. Technol. 181 (2019) 107714, https://doi.org/10.1016/j.compscitech.2019.107714.
[29] V.D. Punetha, Y.M. Ha, Y.O. Kim, Y.C. Jung, J.W. Cho, Rapid remote actuation in shape memory hyperbranched polyurethane composites using cross-linked photothermal reduced graphene oxide networks, Sensor. Actuat. B-Chem. 321 (2020) 128468, https://doi.org/10.1016/j.snb.2020.128468.
[30] Y. Chen, M. Zhang, Z. Lin, X. Shi, Fast near-infrared light responsive shape memory composites: Polydopamine nanospheres hybrid polynorbornene, Polymer 206 (2020) 122898, https://doi.org/10.1016/j.polymer.2020.122898.
[31] G. Zhao, Y. Zhou, J. Wang, Z. Wu, H. Wang, H. Chen, Self-Healing of Polarizing Films via the Synergy between Gold Nanorods and Vitrimer, Adv. Mater. 31 (18) (2019) 1900363, https://doi.org/10.1002/adma.v31.1810.1002/adma.201900363.
[32] S. Chen, J. Ban, L. Mu, H. Zhuo, Development of liquid crystalline polyurethane composites with stage-responsive shape memory effects, Polym. Chem. 9 (5) (2018) 576–583.
[33] S. Zhang, L. Pan, L. Xia, Y. Sun, X. Liu, Dynamic polysulfide shape memory networks derived from elemental sulfur and their dual thermo-/photo-induced solid-state plasticity, React. Funct. Polym. 121 (2017) 8–14.
[34] A.S. Kuenstler, K.D. Clark, J. Read de Alaniz, R.C. Hayward, Reversible Actuation via Photoisomerization-Induced Melting of a Semicrystalline Poly(Azobenzene), ACS Macro Lett. 9 (6) (2020) 902–909.
[35] Y. Wu, Z. Hu, H. Huang, Y. Chen, The design of triple shape memory polymers with stable yet tunable temporary shapes by introducing photo-responsive units into a crystalline domain, Polym. Chem. 10 (12) (2019) 1537–1543.
[36] F. Pilate, R. Mincheva, J. De Winter, P. Gerbaux, L. Wu, R. Todd, J.-M. Raquez, P. Dubois, Design of Multistimuli-Responsive Shape-Memory Polymer Materials by Reactive Extrusion, Chem. Mater. 26 (20) (2014) 5860–5867.
[37] J.Q. Liao, M. Yang, Z. Liu, H.L. Zhang, Fast photoinduced deformation of hydrogenbonded supramolecular polymers containing a-cyanostilbene derivative, J. Mater. Chem. A 7 (2019) 2002–2008.
[38] G. Davidson-Rozenfeld, L. Stricker, J. Simke, M. Fadeev, M. Vázquez-González, B. J. Ravoo, I. Willner, Light-responsive arylazopyrazole-based hydrogels: their applications as shape-memory materials, self-healing matrices and controlled drug release systems, Polym. Chem. 10 (30) (2019) 4106–4115.
[39] Q. Chen, X. Yu, Z. Pei, Y. Yang, Y. Wei, Y. Ji, Multi-stimuli responsive and multi-functional oligoaniline-modified vitrimers, Chem. Sci. 8 (1) (2017) 724–733.
[40] Z. Li, G. Davidson-Rozenfeld, M. Vázquez-González, M. Fadeev, J. Zhang, H. e. Tian, I. Willner, Multi-triggered Supramolecular DNA/Bipyridinium Dithienylethene Hydrogels Driven by Light, Redox, and Chemical Stimuli for Shape-Memory and Self-Healing Applications, J. Am. Chem. Soc. 140 (50) (2018) 17691–17701.
[41] C. Lin, D. Sheng, X. Liu, S. Xu, F. Ji, L.i. Dong, Y. Zhou, Y. Yang, NIR induced self-healing electrical conductivity polyurethane/graphene nanocomposites based on Diels-Alder reaction, Polymer 140 (2018) 150–157.

[42] W. Du, Y. Jin, L. Shi, Y. Shen, S. Lai, Y. Zhou, NIR-light-induced thermoset shape memory polyurethane composites with self-healing and recyclable functionalities, Compos. Part B-Eng. 195 (2020) 108092, https://doi.org/10.1016/j.compositesb.2020.108092.

[43] X. Pang, J. Lv, C. Zhu, L. Qin, Y. Yu, Photodeformable Azobenzene-Containing Liquid Crystal Polymers and Soft Actuators, Adv. Mater. 31 (52) (2019) 1904224, https://doi.org/10.1002/adma.v31.5210.1002/adma.201904224.

[44] L. Zhou, Q. Liu, X. Lv, L. Gao, S. Fang, H. Yu, Photoinduced triple shape memory polyurethane enabled by doping with azobenzene and GO, J. Mater. Chem. C 4 (42) (2016) 9993–9997.

[45] Z. Li, X. Zhang, S. Wang, Y. Yang, B. Qin, K.e. Wang, T. Xie, Y. Wei, Y. Ji, Polydopamine coated shape memory polymer: enabling light triggered shape recovery, light controlled shape reprogramming and surface functionalization, Chem. Sci. 7 (7) (2016) 4741–4747.

[46] X. Li, K. Wang, D.i. Liu, L. Lin, J. Pang, Poly(arylene ether ketone) with tetra quaternary ammonium carbazole derivative pendant for anion exchange membrane, Polymer 195 (2020) 122456, https://doi.org/10.1016/j.polymer.2020.122456.